Optics and Spectroscopy, 2025, Vol. 133, No. 2

02

Luminescence of lanthanide(III) sulfate crystals under photo-, X-ray and triboexcitation

© A.A. Tukhbatullin, N.A. Panova, G.L. Sharipov

Institute of Petrochemistry and Catalysis, Ufa Federal Research Center of the Russian Academy of Sciences,
Ufa, Russia

e-mail: adiska0501@gmail.com

Received May 22, 2024
Revised October 01112024
Accepted December 21, 2025

The comparative studies of the luminescent characteristics (photo-, x-ray excited, triboluminescence spectra, lifetime of excited states and quantum yield of photoluminescence) of crystalline hydrates of lanthanide(III) sulfates (Ce, Pr, Sm, Eu, Gd, Tb, Dy) were carried out. The positions of the Ln(III) ions bands in the triboluminescence spectra of the studied compounds coincide with the positions in the photo- and x-ray excited luminescence spectra, which indicates the identity of the luminescence emitters. It has been shown that the triboluminescence spectrum of inorganic lanthanide salts in the air atmosphere is caused by gas (emitter N_2) and solid-state (emitter - Ln(III)) components. The excitation of Ln^{3+} triboluminescence occurs according to the type of electroluminescence, namely due to the separation and recombination of charge carriers in the electric field of the crystal volume.

Keywords: lanthanide(III) sulfates, photoluminescence, x-ray excited luminescence, triboluminescence, quantum yield, lifetime.

DOI: 10.61011/EOS.2025.02.61019.6726-24

Introduction

Currently, many luminescent devices are based on lanthanide complexes with organic ligands or inorganic crystallophosphores doped with trivalent lanthanide ions [1–10]. The use of such composite materials is associated with the need to ensure a high luminescence intensity of Ln(III) ions. One of the advantages of using not one but many ions of different lanthanides in these compositions is also the possibility of covering them with characteristic spectra of a wide range of wavelengths from ultraviolet (UV, ~ 220 nm) to infrared (~ 750 nm) [11,12]. Lanthanide crystal phosphors and organometallic complexes are obtained mainly using simple oxides and inorganic lanthanide salts [13–16], most of which do not have high luminescence yields and are not used in luminescent devices and analytical techniques. Nevertheless, it has been shown that intense triboluminescence (TL) with a complex spectral composition consisting of a gaseous (luminescence N_2 in the UV region) and solid-state (luminescence centers Ln^{3+}) component is observed in mechanically ground lanthanide sulfate crystals [17]. It has been found that the intensity of TL in the atmosphere of inert gases increases, and the release of hydrocarbon gases leads to the extinguishing of lines N_2, while lines of atoms of inert gases and light-emitting products (*CH and $^*C_2$) mechanochemical decomposition reactions of hydrocarbon gases [18]. A glow was also detected in Ref. [19–21] that occurs in case of ultrasonic treatment of the suspension (sonotriboluminescence, STL). Crystals of terbium(III) and europium(III) sulfates were used as the suspension base. The knowledge about the spectral-luminescent characteristics of phosphors obtained in the field of TL and STL lanthanide sulfates, as well as their luminescence with other excitation methods, will be of undoubted interest for the development of new technological processes and analytical applications in optical spectroscopy. Meanwhile, comparative systematic studies of the luminescence of a number of lanthanide sulfates with different methods of its excitation, despite obtaining certain knowledge and skills in this field of luminescence, have not been conducted before.

In this regard, detailed comparative studies of luminescence $Ln_2(SO_4)_3 \cdot 8H_2O$ (Ln=Ce, Pr, Sm, Eu, Gd, Tb, Dy) in case of photo-, X-ray, and triboexcitation have been conducted in this paper. The full spectral and luminescent characteristics were evaluated and obtained: TL, X-ray excited luminescence (XEL), photoluminescence (PL) spectra and their excitation spectra, the lifetime of excited states of Ln^{3+} ions in crystals, and the quantum yields of their photoluminescence.

Experimental part

$Ln_2(SO_4)_3 \cdot 8H_2O$ (Ln=Ce, Pr, Sm, Eu, Gd, Tb, Dy) of „CP“(chemically pure) grade were used to study luminescence. The crystals, crushed to a powdery state (250 mg, average particle size $\sim 100\,\mu$m), were placed in a tightly closed cylindrical steel cuvette with a diameter of 20 mm with a quartz window at the bottom [22,23].

To obtain TL, a stirrer made of a fluoroplastic tube, which was driven by an electric motor at 1000 rpm, was used to grind crystals along the bottom of the cuvette. TL was also excited using UZDN-2T ultrasonic system (22 kHz) with a titanium waveguide with its tip was in direct contact with the crystal layer inside the cuvette [19,20].

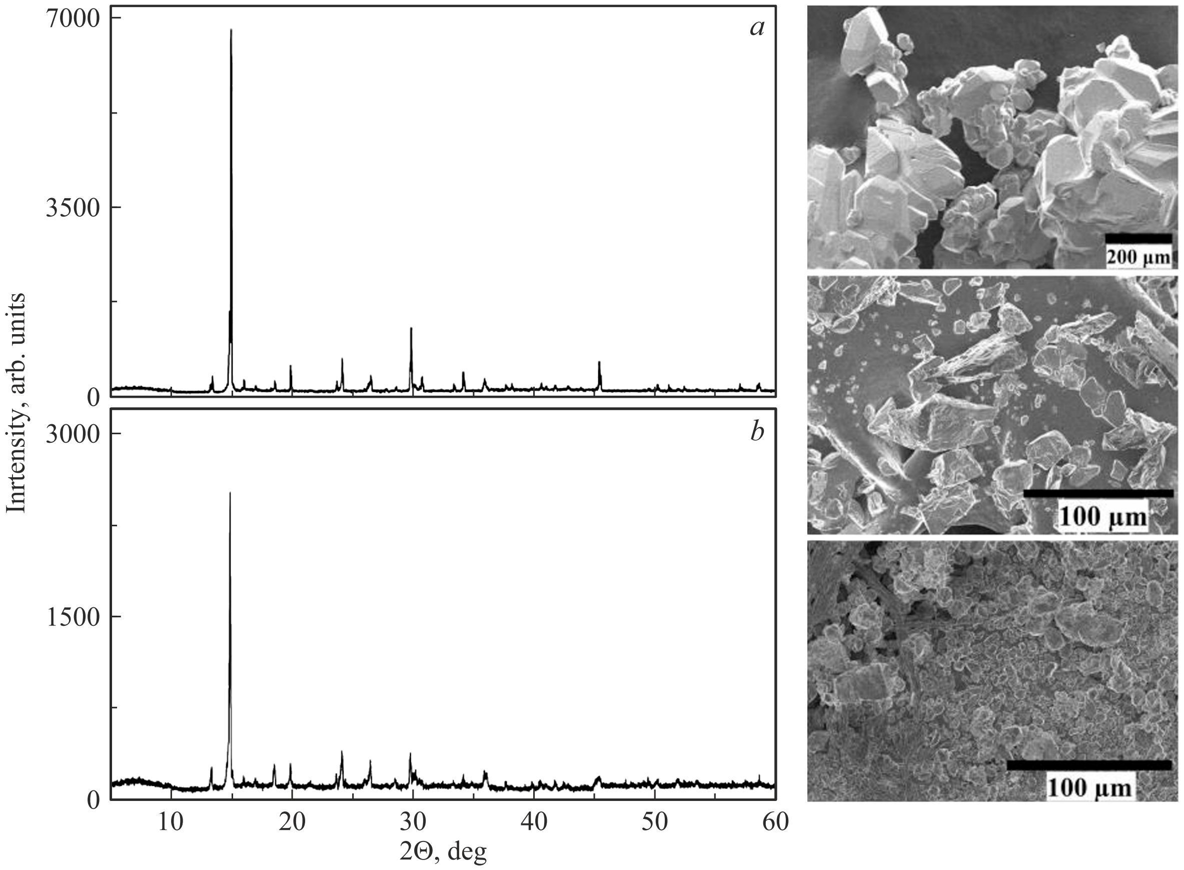

Figure 1. X-ray diffraction patterns of samples $Tb_2(SO_4)_3 \cdot 8H_2O$ (*a*) before and (*b*) after machining. SEM image of particles (*c*) before and (*d*) after mechanical grinding of crystals $Tb_2(SO_4)_3 \cdot 8H_2O$, (*e*) after ultrasonic treatment of crystals $Gd_2(SO_4)_3 \cdot 8H_2O$.

The XEL crystals were excited using BSM-1 microfocus X-ray tube with an anode copper mirror with a voltage up to 45 kV [24]. The glow was recorded in an atmospheric atmosphere at room temperature (298 K).

The spectra of PL excitation, X-ray excited and triboluminescence, the lifetime of the excited state, and the quantum yield of PL were recorded using Fluorolog-3 and Zolix OmniFluo-900 spectrofluorimeters. When studying the excitation spectra, PL, lifetime, and quantum yield, the crystals were placed in a holder for solid-state samples that were exposed to exciting radiation (xenon lamp 450,W Fluorolog-3 and 75,W Zolix) or pulsed LEDs NanoLED (pulse duration < 1.2 ns), CNI Laser diode lasers (pulse duration 0.02–1 ns, depending on repetition rate).

The quantum yields of PL were evaluated using an integrating sphere used to determine the absolute quantum yield on a Zolix spectrofluorimeter.

The luminescence spectra were corrected in all cases using standard instrument correction. Spectral data and time characteristics of luminescence were processed using spectrofluorimeter software.

The morphology of microcrystals was studied by scanning electron microscopy (SEM) using a Hitachi Regulus SU 8220 (FE-SEM) electron microscope. The SEM images were recorded in the secondary electron recording mode with an accelerating voltage of 2 kV.

X-ray diffraction analysis of lanthanide(III) sulfate powders was performed using Shimadzu XRD-7000 diffractometer with CuK_α-radiation. Scanning was performed in the range of angles 2θ from 5° to 60° with 1 deg/min rate.

Results and discussion

Previously, the PL, XEL, and TL of cerium, europium, and terbium sulfates were studied sporadically [17]. The luminescence in case of different methods of excitation of sulfates of most other lanthanides has been poorly studied. For example, there is no information in the literature about the XEL of crystals of gadolinium, praseodymium, dysprosium, and samarium sulfates. Only recently, TL of Sm^{3+} was discovered when crystals of samarium sulfate were exposed to ultrasonic waves [25]. Comparative information has been obtained in this report about the spectral and luminescent characteristics of sulfate crystallohydrates of seven lanthanide(III) ions, which emit characteristic light in the UV and visible regions of the spectrum at PL, XEL and TL and have sufficiently high quantum yields of PL.

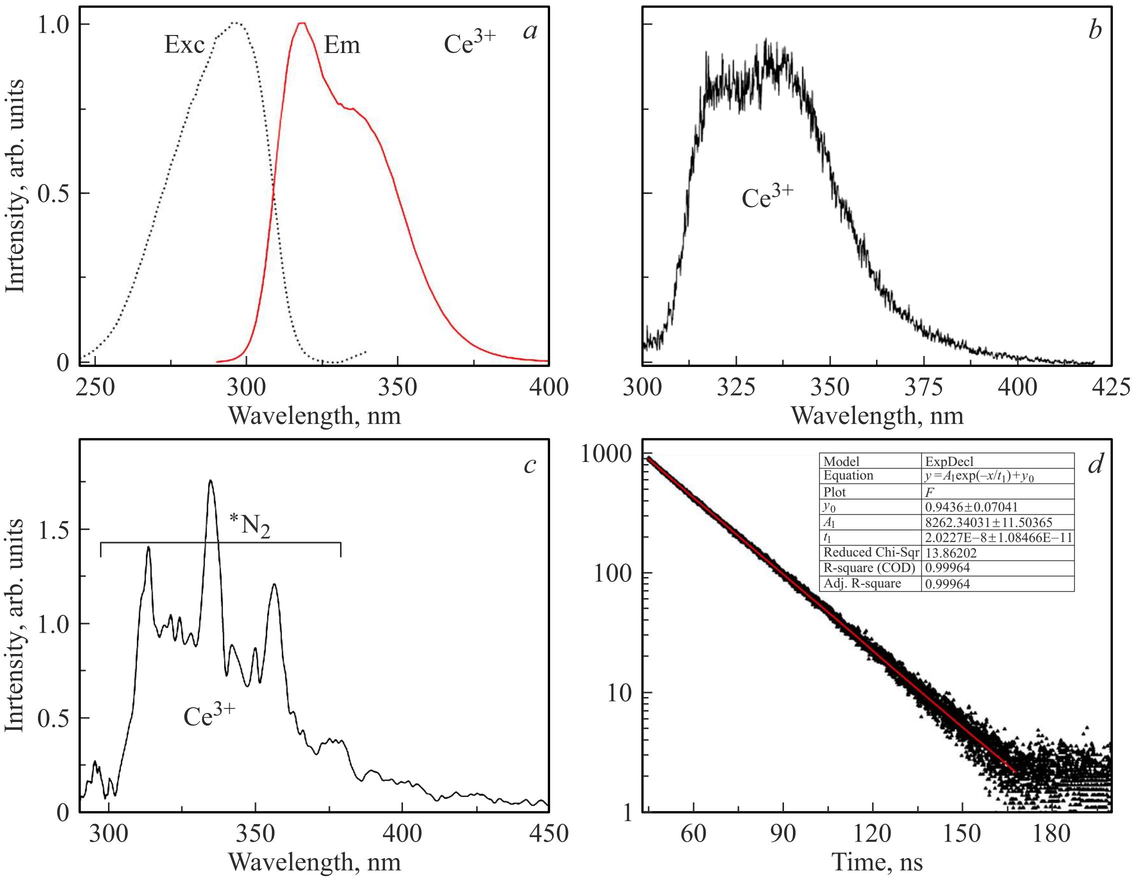

Model	ExpDecl
Equation	$y=A_1\exp(-x/t_1)+y_0$
Plot	F
y_0	0.9436±0.07041
A_1	8262.34031±11.50365
t_1	2.0227E−8±1.08466E−11
Reduced Chi-Sqr	13.86202
R-square (COD)	0.99964
Adj. R-square	0.99964

Figure 2. Spectra $Ce_2(SO_4)_3 \cdot 8H_2O$: (*a*) excitations of PL (dotted line, $\lambda_{\text{lum}} = 330$ nm) and PL (solid line, $\lambda_{\text{exc}} = 290$ nm), $\Delta\lambda = 0.5$ nm; (*b*) XEL, Xray, 45 keV, $\Delta\lambda = 1$ nm; (*c*) TL, $\Delta\lambda = 2$ nm. (*d*) Kinetics of luminescence decay Ce^{3+} with pulse excitation NanoLED-280 ($\lambda_{\text{exc}} = 288$ nm, $\lambda_{\text{lum}} = 335$ nm).

It should be noted that lanthanide sulfate crystallohydrates crystallize isostructurally in the monoclinic space group $C2/c$ [26–32]. Lanthanide atoms are coordinated with eight O atoms (four oxygen atoms of the sulfate group and four water molecules). All water molecules are located in an internal coordination sphere and are bound to lanthanide atoms.

Based on the results of X-ray diffraction analysis of the studied powders and literature data, it was revealed that mechanical action (including ultrasonic powder treatment) does not lead to a significant change in the crystal structure. For example, Fig. 1, *a, b* shows X-ray diffraction patterns of terbium(III) sulfate powders before and after grinding the crystals with a stirrer. A slight broadening of the peaks and a decrease of their intensity are observed after mechanical grinding of the powder layer [25], which mainly indicates a decrease of the particle size in the crystalline phase. Indeed, while lanthanide salts have an average crystal size of $100-500\,\mu$m before grinding, these microcrystals have an average size of about $10-30\,\mu$m after mechanical grinding, and their size is $5-10\,\mu$m after ultrasonic treatment (Fig. 1, *c, d, e*).

Photoluminescence

The luminescence of the studied crystals $Ln_2(SO_4)_3 \cdot 8H_2O$ collectively covers the spectral range from ~ 220 to ~ 750 nm (Fig. 2–8, *a*). In the PL spectra, the luminescence of Ce^{3+} ions (Fig. 2, *a*) and Pr^{3+} (Fig. 3, *a*) is attributable to transitions from $5d$ to $4f$-shell, which are characterized by intense wide bands in the UV region of the spectrum.

In case of photoexcitation of cerium(III) sulfate crystals, a broad maximum at 320 nm and a shoulder at 336 nm are observed, attributed to transitions from the $5d^1$-level to $^2F_{7/2}$ and $^2F_{5/2}$-levels of the spin-orbit-split $4f^1$-ground state [33–36]. UV luminescence of Pr^{3+} is associated with intra-configuration transitions from the lower excited $4f^15d^1$-level to the multiplets $^3H_{4,5,6}$, $^3F_{2,3,4}$ and $^1G_4$ of the ground $4f^2$- state [33,37–39]. The main maxima of Sm^{3+} ion (Fig. 4, *a*) corresponding to transitions from the $^4G_{5/2}$- level to $^6H_{5/2,7/2,9/2,11/2}$ level are recorded in the PL spectrum of $Sm_2(SO_4)_3 \cdot 8H_2O$ crystals as well as the less intense maxima of 781 nm ($^4G_{5/2} \rightarrow {}^6H_{13/2}$), 860–940 nm ($^4G_{5/2} \rightarrow {}^6F_{j/2}$) [25,40,41].

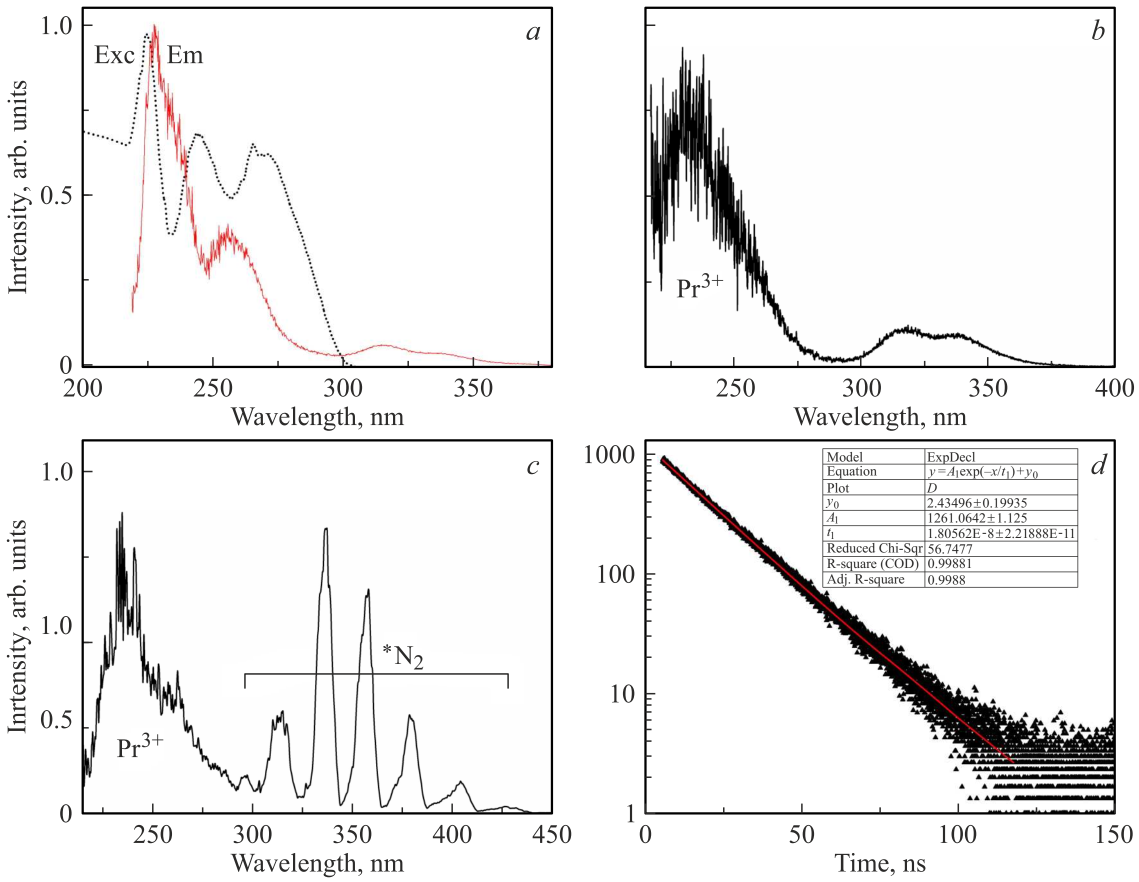

Figure 3. Spectra $Pr_2(SO_4)_3 \cdot 8H_2O$: (*a*) excitations of PL (dotted line, $\lambda_{\text{lum}} = 325$ nm) and PL (solid line, $\lambda_{\text{exc}} = 215$ nm), $\Delta\lambda = 1$ nm; (*b*) XEL, Xray, 45 keV, $\Delta\lambda = 2$ nm; (*c*) TL, $\Delta\lambda = 3$ nm. (*d*) Kinetics of luminescence decay Pr^{3+} with pulsed excitation NanoLED-265 ($\lambda_{\text{exc}} = 268$ nm, $\lambda_{\text{lum}} = 315$ nm).

Several maxima are observed (Fig. 5, *a*) in case of photoexcitation of europium(III) sulfate corresponding to transitions from $^5D_0$- and $^5D_1$-levels to $^7F_{0-6}$ levels [42–44]. It should be noted that the intensity of the glow from the $^5D_1$-level is rather weak due to rapid nonradiative deactivation from the $^5D_1$-level to the $^5D_0$-level.

The PL of gadolinium(III) sulfate is recorded in the UV region of the spectrum (Fig. 6, *a*), the main maximum is observed at 311 nm ($^6P_{7/2} \rightarrow {}^8S_{7/2}$), a less intense maximum is observed at 305 nm ($^6P_{5/2} \rightarrow {}^8S_{7/2}$) [45,46].

Photoexcitation of terbium(III) sulfate results in intense luminescence maxima in the visible region of the spectrum (Fig. 7, *a*) attributable to transitions $^5D_4 \rightarrow {}^7F_{0-6}$ [21,47,48].

The PL of dysprosium(III) sulfate is also detected in the visible region of the spectrum (Fig. 8, *a*) (transitions $^4F_{9/} \rightarrow {}^6H_{15/2,13/2,11/2,9/2}$ [49–51]).

The PL excitation spectra for all studied lanthanide sulfates are shown in Fig. 2–8, it a. The kinetics of luminescence decay for all the studied compounds is described by a single exponent (Fig. 2–8, *d*), which indicates the uniformity of the crystal structure, the absence of impurities and defects in the crystals. Long excited state lifetimes are characteristic of gadolinium ions (Fig. 6, *d*), europium (Fig. 5, *d*) and terbium (Fig. 7, *d*) with forbidden *f*-*f*-transitions, on the contrary, cerium and praseodymium ions (*d*-*f*-transitions) are characterized by short lifetimes (Fig. 2, *d* and 3, *d*) and high PL quantum yields. For comparison, the PL quantum yield of anthracene (often used as a reference [52,53]) was estimated using this setup. The PL quantum yields coincide with the literature data and amounted to 24 % for 10^{-4} mol/L solution and 28 % for anthracene powder.

X-ray excited luminescence and triboluminescence

The positions of lanthanide ion bands in the XEL (Fig. 2–8, it b) and TL spectra (Fig. 2–8, it with) of lanthanide(III) sulfates coincide with the positions in the PL spectra. In the case of TL, the presence of molecular nitrogen lines in the UV region makes it difficult to accurately identify the position of the maxima of the Gd^{3+} ion. The lines N_2 for the Ce^{3+} ion are recorded against the background of the cerium(III) band (Fig. 2, *c*). It was shown in Ref. [25] that in case of mechanical grinding of crystals, the absence of TL $Sm_2(SO_4)_3 \cdot 8H_2O$ (along with the low quantum yield of

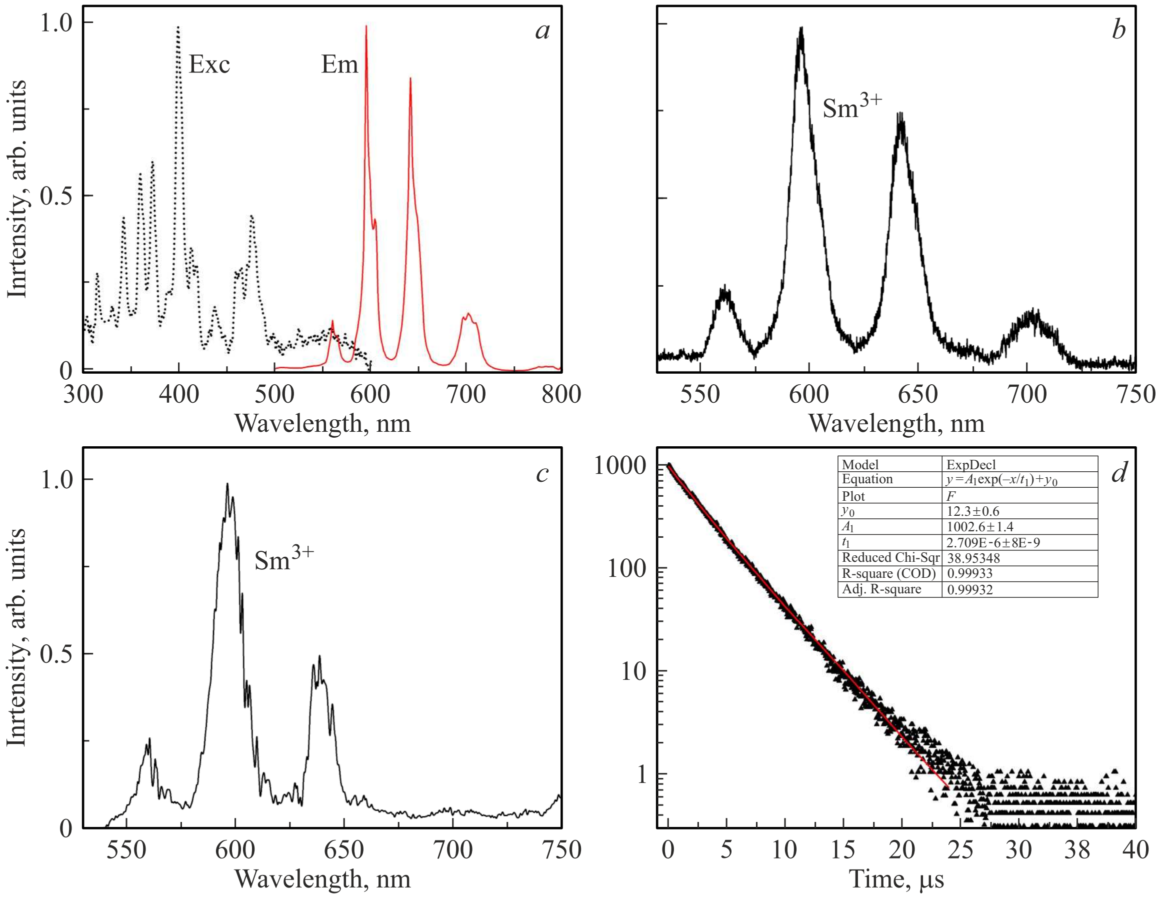

Model	ExpDecl
Equation	$y=A_1\exp(-x/t_1)+y_0$
Plot	F
y_0	12.3±0.6
A_1	1002.6±1.4
t_1	2.709E-6±8E-9
Reduced Chi-Sqr	38.95348
R-square (COD)	0.99933
Adj. R-square	0.99932

Figure 4. Spectra $Sm_2(SO_4)_3 \cdot 8H_2O$: (*a*) excitations of PL (dotted line, $\lambda_{\text{lum}} = 640$ nm) and PL (solid line, $\lambda_{\text{exc}} = 405$ nm), $\Delta\lambda = 1$ nm; (*b*) XEL, Xray, 45 keV, $\Delta\lambda = 2$ nm; (*c*) TL under ultrasonic exposure (22 kHz, 15 W), $\Delta\lambda = 4$ nm. (*d*) Kinetics of luminescence decay of Sm^{3+} under pulsed excitation CNI Laser ($\lambda_{\text{exc}} = 405$ nm, $\lambda_{\text{lum}} = 600$ nm).

Sm^{3+}) is also associated with weak pressure on the crystals and a low rate of mechanical grinding (1–2 m/s).

The ultrasonic treatment of samarium sulfate crystals made it possible to excite its TL with the identification of the main spectral components of the luminescence N_2 and Sm^{3+}. Experiments have shown that ultrasonic exposure significantly increases the intensity of TL, in the case of terbium sulfate, the intensity increased by ~ 40 times compared with mechanical grinding using a stirrer [25]. The bright glow makes it possible to record TL spectra with high resolution, which makes it possible, for example, to clearly separate narrow lines of N_2 and quasi-lines of Gd^{3+} (Fig. 6, *c*). The high intensity of TL is ensured by an increase of the number of cycles of mechanical action of the end of the ultrasonic waveguide on the crystal layer per second by more than 1000 times compared with cycles of action during grinding with a fluoroplastic mixer. Ultrasonic treatment leads to high-speed collisions of crystals in the reactor with intense crystal destruction, formation of fine particles and an increase in the area of the active surface. This leads to an increase of the TL intensity. For example, it was shown in [54] that the intensity of TL is directly proportional to the area of freshly formed surfaces occurring during crystal destruction. Previously, the ultrasonic method was not used to excite TL, however, as can be seen, this method allows for a more detailed study of the spectral characteristics of TL.

Despite the fact that lanthanide sulfates have a complex TL spectral composition, the mechanisms of excitation of luminescence of N_2 and Ln^{3+} ions differ. Luminescence of N_2 (coinciding with the spectrum of discharges in an atmosphere of molecular nitrogen) occurs as a result of discharges formed between differently charged microcrack walls or crystal surfaces [17,55]. Ln^{3+} ions are located in the crystal volume, therefore, their luminescence is excited by ultrasonic waves mainly due to the separation and recombination of charge carriers in the electric field of the crystal layer [17,23,55,56].

Comparative analysis

For convenience of comparison, the spectral-luminescent characteristics of lanthanide sulfates at PL, XEL and TL are summarized in the following table. It should be noted that lanthanide sulfate crystallohydrates contain eight

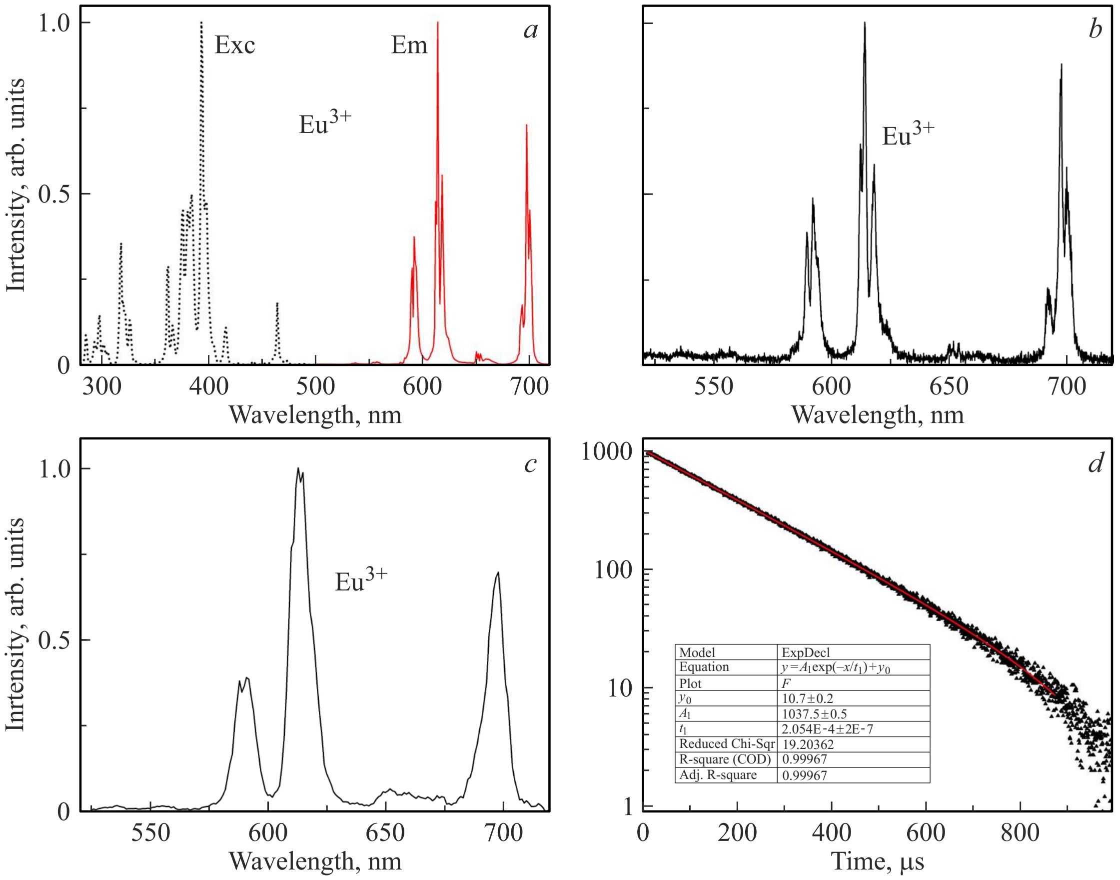

Figure 5. Spectra $Eu_2(SO_4)_3 \cdot 8H_2O$: (*a*) excitations of PL (dotted line, $\lambda_{\text{lum}} = 614$ nm) and PL (solid line, $\lambda_{\text{exc}} = 395$ nm), $\Delta\lambda = 1$ nm; (*b*) XEL, Xray, 45 keV, $\lambda = 2$ nm; (*c*) TL, $\lambda = 4$ nm. (*d*) Kinetics of luminescence decay Eu^{3+} with pulsed excitation CNI Laser ($\lambda_{\text{exc}} = 375$ nm, $\lambda_{\text{lum}} = 614$ nm).

Spectral and luminescent characteristics of lanthanide(III) sulfates

Salts	PL, XEL, TL, $\lambda_{\max}$(nm)	Lifetime, τ (μs)	PL quantum yield φ(%)	Triboluminescence	
				Grinding by stirrer	US impact
$Ce_2(SO_4)_3 \cdot 8H_2O$	320, 336	0.020 ± 0.001	72.4	+	+
$Pr_2(SO_4)_3 \cdot 8H_2O$	227, 234, 255, 315, 334	0.018 ± 0.001	71.2	+	+
$Sm_2(SO_4)_3 \cdot 8H_2O$	560, 595, 640, 700	2.7 ± 0.07	0.5	−	+
$Eu_2(SO_4)_3 \cdot 8H_2O$	592, 614, 651, 698	205 ± 6	6.3	+	+
$Gd_2(SO_4)_3 \cdot 8H_2O$	305, 311	3160 ± 85	10.5	+	+
$Tb_2(SO_4)_3 \cdot 8H_2O$	490, 543, 589, 620	707 ± 25	17.1	+	+
$Dy_2(SO_4)_3 \cdot 8H_2O$	480, 571, 660, 750	2.4 ± 0.07	2.1	+	+

water molecules in the coordination sphere of the Ln(III) ion. Therefore, in most cases, for ions with luminescent f-f-transitions (Sm, Eu, Gd, Tb, Dy), the low quantum yield and relatively short lifetime for forbidden transitions are associated with nonradiative deactivation as a result of the transfer of excitation energy to high-frequency vibrations of OH-groups of water molecules [40.57]. The effect of H_2O molecules on luminescent characteristics has been studied in detail in a number of papers [47,58,59].

Conclusion

It is shown that the positions of the maxima of the lanthanide ion bands in the PL, XEL, and TL spectra of the studied lanthanide(III) sulfate crystals coincide, which indicates the equivalence of the composition of the luminescence centers.

Ultrasonic treatment of the crystal layer was used to excite intense TL. The use of ultrasound greatly increases

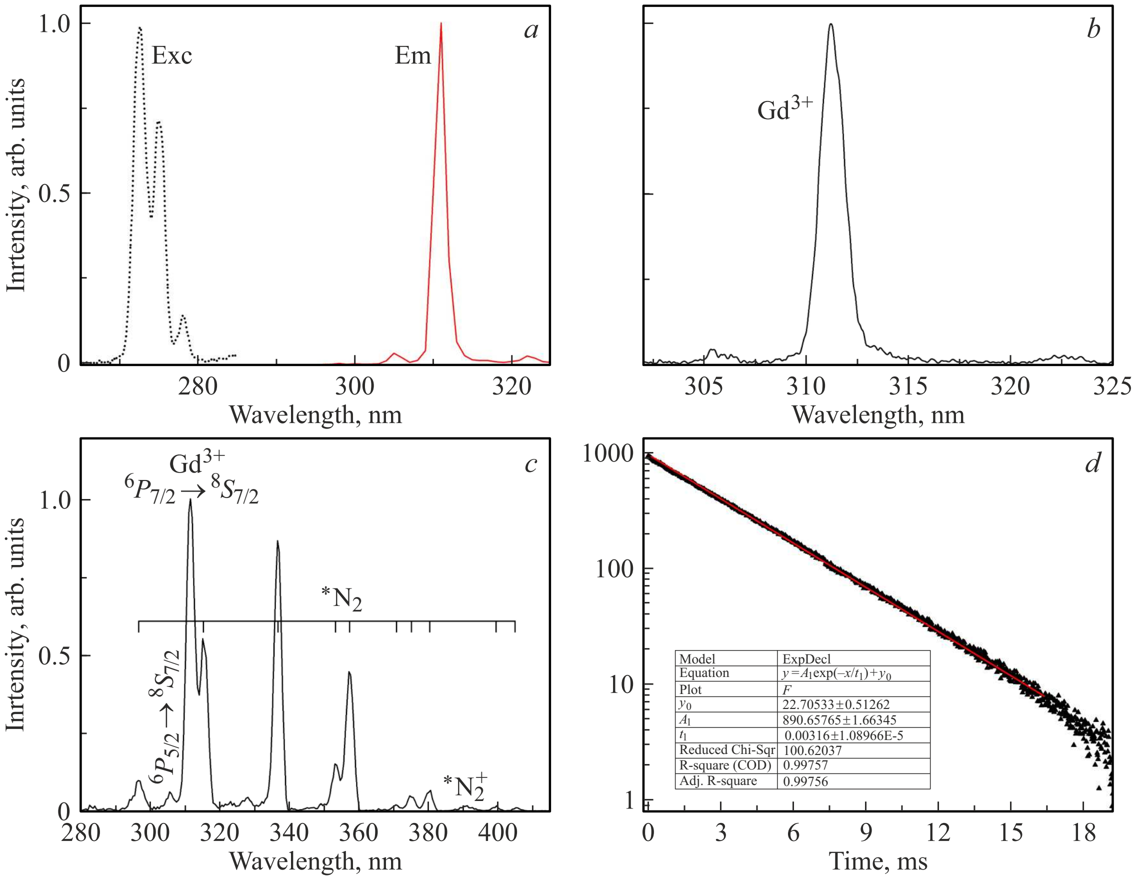

Model	ExpDecl
Equation	$y = A_1 \exp(-x/t_1) + y_0$
Plot	F
y_0	22.70533±0.51262
A_1	890.65765±1.66345
t_1	0.00316±1.08966E-5
Reduced Chi-Sqr	100.62037
R-square (COD)	0.99757
Adj. R-square	0.99756

Figure 6. Spectra $Gd_2(SO_4)_3 \cdot 8H_2O$: (*a*) excitations of PL (dotted line, $\lambda_{\text{lum}} = 311$ nm) and PL (solid line, $\lambda_{\text{exc}} = 272$ nm), $\Delta\lambda = 1$ nm; (*b*) XEL, Xray, 45 keV, $\Delta\lambda = 2$; (*c*) TL under ultrasonic exposure (22 kHz, 15 W), $\Delta\lambda = 1$ nm. (*d*) Kinetics of Gd^{3+} luminescence decay in case of pulsed excitation by a xenon lamp ($\lambda_{\text{exc}} = 272$ nm, $\lambda_{\text{lum}} = 311$ nm).

the speed and intensity of mechanical treatment of crystals, resulting in a stable and bright luminescence sufficient to record the TL spectrum with high spectral resolution. The luminescence in case of lanthanide salt crystal tribolysis is excited like the electroluminescence of phosphors, namely it is caused by the separation and recombination of charge carriers in the electric field of the crystal layer that takes place in case of mechanical treatment. The development of sensors for the destruction of structural materials is an attractive area for application of TL of lanthanide sulfates owing to its intensity.

Acknowledgments

The microcrystals were analyzed using the equipment of „Agidel" Center of Institute of Petrochemisty and Catalysis of Ufa Federal Research Centre of the Russian Academy of Sciences, RAS.

Funding

This study was supported by a grant from the Russian Science Foundation (project /No 23-12-20002, https://rscf.ru/project/23-12-20002/).

Conflict of interest

The authors declare that they have no conflict of interest.

References

[1] Y. Yu, G. Chen, Y. Zhou, Z. Han. J. Rare Earth., **33**, 453 (2015). DOI: 10.1016/S1002-0721(14)60440-3

[2] J.-C.G. Bünzli. Coord. Chem. Rev., **293–294**, 19 (2015). DOI: 10.1016/j.ccr.2014.10.013

[3] Q. Li, B. Yan. J. Rare Earth., **37**, 113 (2019). DOI: 10.1016/j.jre.2018.10.001

[4] V. Balaram. Geoscience Frontiers, **10**, 1285 (2019). DOI: 10.1016/j.gsf.2018.12.005

[5] I. Gupta, S. Singh, S. Bhagwan, D. Singh. Ceram. Int., **47**, 19282 (2021). DOI: 10.1016/j.ceramint.2021.03.308

[6] A.A. Ansari, M.R. Muthumareeswaran, R. Lv. Coord. Chem. Rev., **466**, 214584 (2022). DOI: 10.1016/j.ccr.2022.214584

[7] H. Li, Y. Chen, T. Wang, L. Liu, B. Zhang, Y. Wang, D. Yang. J. Colloid. Interface Sci., **670**, 530 (2024). DOI: 10.1016/j.jcis.2024.05.110

[8] R.-K. Du, X.-L. He, T.-Z. Xiao, Y.-F. Xiang, L. Zhong, L. Zhou, J.-C. Zhang, D.-Q. Yao, T.-Y. Sun, M.-M. Wu. Laser Photonics Rev., 2401211 (2024). DOI: 10.1002/lpor.202401211

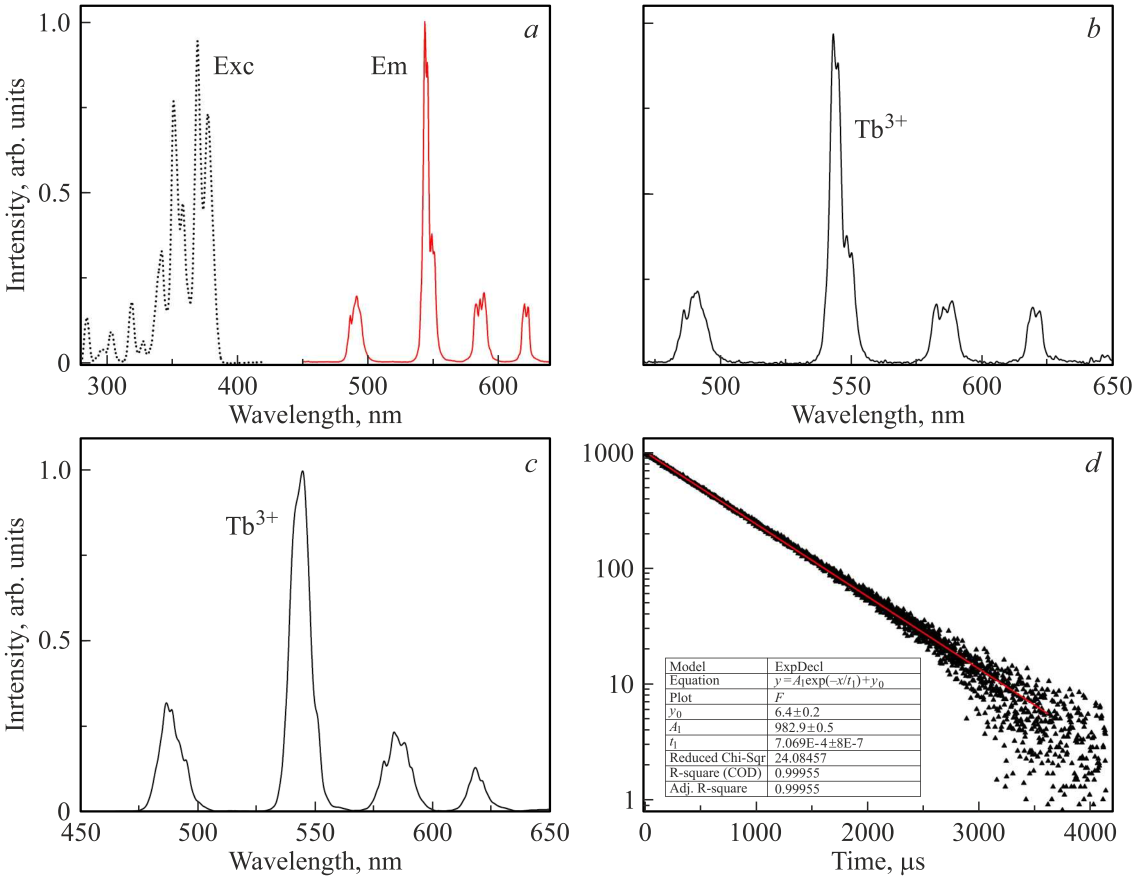

Model	ExpDecl
Equation	$y=A_1\exp(-x/t_1)+y_0$
Plot	*F*
y_0	6.4±0.2
A_1	982.9±0.5
t_1	7.069E-4±8E-7
Reduced Chi-Sqr	24.08457
R-square (COD)	0.99955
Adj. R-square	0.99955

Figure 7. Spectra $Tb_2(SO_4)_3\cdot 8H_2O$: (*a*) excitations of PL (dotted line, $\lambda_{\text{lum}} = 544$ nm) and PL (solid line, $\lambda_{\text{exc}} = 350$ nm), $\Delta\lambda = 1$ nm; (*b*) XEL, Xray, 45 keV, $\Delta\lambda = 1$ nm; (*c*) TL, $\Delta\lambda = 1$ nm. (*d*) Kinetics of luminescence decay Tb^{3+} with pulse excitation CNI Laser ($\lambda_{\text{exc}} = 375$ nm, $\lambda_{\text{lum}} = 544$ nm).

[9] D. Yang, H. Li, H. Li. Coord. Chem. Rev., **514**, 215875 (2024). DOI: 10.1016/j.ccr.2024.215875

[10] H. Yang, Y. Wei, H. Ju, X. Huang, J. Li, W. Wang, D. Peng, D. Tu, G. Li. Adv. Mater., **36**, 2401296 (2024). DOI: 10.1002/adma.202401296

[11] W. Li, Y. Cai, J. Chang, J. Liu, S. Wang, J.-C. Zhang. Adv. Funct. Mater., 2412494 (2024). DOI: 10.1002/adfm.202412494

[12] S. Chang, K. Zhang, D. Peng, Y. Deng, C.-X. Shan, L. Dong. Nano Energy, **122**, 109325 (2024). DOI: 10.1016/j.nanoen.2024.109325

[13] B.V. Bukvetskii, A.S. Shishov, A.G. Mirochnik. Russ. Chem. Bull., **72**, 1307 (2023). DOI: 10.1007/s11172-023-3906-y.

[14] B.V. Bukvetskii, I.V. Kalinovskaya. Luminescence, **39**, e4617 (2024). DOI: 10.1002/bio.4617

[15] Y. Hirai, S. Van Baaren, T. Ohmura, T. Nakanishi, T. Takeda, Y. Kitagawa, Y. Hasegawa, R. Métivier, C. Allain. Adv. Opt. Mater., **11**, 2203139 (2023). DOI: 10.1002/adom.202203139

[16] B. Vasanthi, N.P. Gopakumar, P.S. Anjana, G. Nair. Luminescence, **39**, e4602 (2024). DOI: 10.1002/bio.4602

[17] *Triboluminescence: Theory, Synthesis, and Application*, ed. by D.O. Olawale, O.O.I. Okoli, R.S. Fontenot, W.A. Hollerman (Springer International Publishing, Cham, 2016). DOI: 10.1007/978-3-319-38842-7

[18] A.A. Tukhbatullin, G.L. Sharipov, D.N. Gerasimov. J. Lumin., **197**, 335 (2018). DOI: 10.1016/j.jlumin.2018.01.038

[19] A.A. Tukhbatullin, G.L. Sharipov, N.F. Burangulova, A.G. Mustafin. Ultrason. Sonochem., **50**, 251 (2019). DOI: 10.1016/j.ultsonch.2018.09.026

[20] A.A. Tukhbatullin, G.L. Sharipov, N.F. Burangulova. J. Mol. Liq., **289**, 110973 (2019). DOI: 10.1016/j.molliq.2019.110973

[21] A.A. Tukhbatullin, G.L. Sharipov. Appl. Spectrosc., **76**, 1216 (2022). DOI: 10.1177/00037028221098442

[22] A.A. Tukhbatullin, G.L. Sharipov, A.A. Galina. Luminescence, **33**, 1180 (2018). DOI: 10.1002/bio.3533

[23] A.A. Tukhbatullin, G.L. Sharipov. Opt. Mater., **109**, 110402 (2020). DOI: 10.1016/j.optmat.2020.110402

[24] V.P. Kazakov, G.L. Sharipov. *Radiolyuminescentsiya vodnykh rastvorov* (Nauka, M, 1986) (in Russian).

[25] A.A. Tukhbatullin, G.L. Sharipov. Opt. Mater., **143**, 114253 (2023). DOI: 10.1016/j.optmat.2023.114253

[26] V.M. Malhotra, H.D. Bist, G.C. Upreti. J. Chem. Phys., **69**, 1919 (1978). DOI: 10.1063/1.436828

[27] V.M. Malhotra, H.D. Bist, G.C. Upreti. Chem. Phys. Lett., **48**, 334 (1977). DOI: 10.1016/0009-2614(77)80327-8

[28] H.-U. Hummel, E. Fischer, T. Fischer, P. Joerg, G. Pezzei. Z. Anorg. Allg. Chem., **619**, 805 (1993). DOI: 10.1002/zaac.19936190429

[29] Y.-Q. Zheng, Y.-J. Zhu, J.-L. Lin. Z. Kristallogr., **217**, 299 (2002). DOI: 10.1524/ncrs.2002.217.1.299

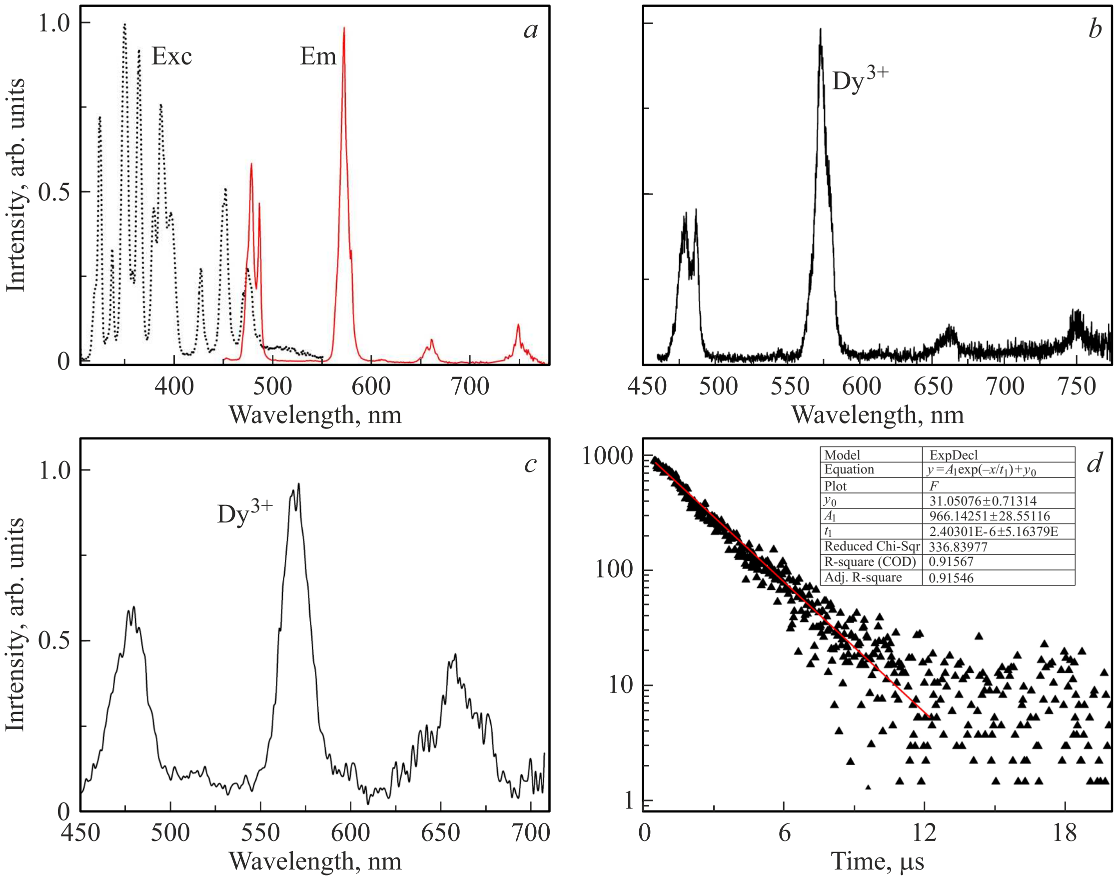

Figure 8. Spectra $Dy_2(SO_4)_3 \cdot 8H_2O$: (*a*) excitation of PL (dotted line, $\lambda_{\text{lum}} = 570\,\text{nm}$) and PL (solid line, $\lambda_{\text{exc}} = 350\,\text{nm}$), $\Delta\lambda = 1\,\text{nm}$; (*b*) XEL, Xray, 45 keV, $\Delta\lambda = 1\,\text{nm}$; (*c*) TL, $\Delta\lambda = 5\,\text{nm}$. (*d*) Kinetics of luminescence decay Dy^{3+} with pulse excitation CNI Laser ($\lambda_{\text{exc}} = 375\,\text{nm}$, $\lambda_{\text{lum}} = 570\,\text{nm}$).

[30] D.-Y. Wei, Y.-Q. Zheng. Z. Kristallogr., **218**, 299 (2003). DOI: 10.1524/ncrs.2003.218.3.277

[31] D.-Y. Wei, Y.-Q. Zheng. Z. Kristallogr., **218**, 23 (2003). DOI: 10.1524/ncrs.2003.218.jg.23

[32] B.M. Casari, V. Langer. Z. Anorg. Allg. Chem., **633**, 1074 (2007). DOI: 10.1002/zaac.200700003

[33] P. Dorenbos. J. Lumin., **91**, 91 (2000). DOI: 10.1016/S0022-2313(00)00197-6

[34] M.P. Tsvirko, A.G. Svetashev. Opt. Mater., **31**, 1842 (2009). DOI: 10.1016/j.optmat.2008.11.025

[35] M.A. Bakane, C.P. Joshi, S.V. Moharil, P.L. Muthal, S.M. Dhopte. Luminescence, **26**, 553 (2011). DOI: 10.1002/bio.1269

[36] R.M. Brewer, M. Nicol. J. Lumin., **23**, 269 (1981). DOI: 10.1016/0022-2313(81)90133-2

[37] V.A. Pustovarov, K.V. Ivanovskikh, Yu.E. Khatchenko, V.Yu. Ivanov, M. Bettinelli, Q. Shi. Phys. Solid State, **61**, 758 (2019). DOI: 10.1134/S1063783419050275.

[38] S.A. Kiselev, V.A. Pustovarov, E.S. Trofimova, M.O. Petrova. Opt. Spectrosc., **131** (5), 568 (2023). DOI: 10.61011/EOS.2023.05.56507.62-22.

[39] A.M. Srivastava, A.A. Setlur, H.A. Comanzo, W.W. Beers, U. Happek, P. Schmidt. Opt. Mater., **33**, 292 (2011). DOI: 10.1016/j.optmat.2010.08.026

[40] G. Stein, E. Würzberg. J. Chem. Phys., **62**, 208 (1975). DOI: 10.1063/1.430264

[41] P. Kaur, S. Kaur, G.P. Singh, D.P. Singh. Solid State Commun., **171**, 22-25 (2013). DOI: 10.1016/j.ssc.2013.07.021

[42] S. Ram. J. Raman Spectrosc., **18**, 537 (1987). DOI: 10.1002/jrs.1250180803

[43] Y.G. Denisenko, A.S. Aleksandrovsky, V.V. Atuchin, A.S. Krylov, M.S. Molokeev, A.S. Oreshonkov, N.P. Shestakov, O.V. Andreev. J. Ind. Eng. Chem., **68**, 109 (2018). DOI: 10.1016/j.jiec.2018.07.034

[44] A.V. Mamykin, G.A. Masyagutova, S.S. Ostakhov, S.L. Khursan. J. Solid State Chem., **290**, 121554 (2020). DOI: 10.1016/j.jssc.2020.121554

[45] D.D. Ramteke, R.S. Gedam. J. Rare Earth., **32**, 389-393 (2014). DOI: 10.1016/S1002-0721(14)60082-X

[46] X. Wang, Y. Chen, P.A. Kner, Z. Pan. Dalton Trans., **50**, 3499-3505 (2021). DOI: 10.1039/D1DT00120E

[47] A.A. Mamykin, A.V. Mamykin, S.S. Ostakhov, V.P. Kazakov. High Energ. Chem., **44**, 109 (2010). DOI: 10.1134/S0018143910020049

[48] P. Netzsch, H. Bariss, L. Bayarjargal, H.A. Höppe. Dalton Trans., **48**, 16377 (2019). DOI: 10.1039/C9DT03436F

[49] R.V. Rodrigues, L. Marciniak, L.U. Khan, J.R. Matos, H.F. Brito, W. Stręk. J. Rare Earth., **34**, 814 (2016). DOI: 10.1016/S1002-0721(16)60099-6

[50] B.V. Bukvetskii, A.G. Mirochnik, P.A. Zhikhareva. Opt. Spectrosc., **126** (3), 195 (2019). DOI: 10.1134/S0030400X19030044

[51] B.V. Bukvetskii, A.G. Mirochnik, P.A. Zhikhareva. Opt. Spectrosc., **128** (3), 323 (2020). DOI: 10.1134/S0030400X20030054

[52] K. Suzuki, A. Kobayashi, S. Kaneko, K. Takehira, T. Yoshihara, H. Ishida, Y. Shiina, S. Oishi, S. Tobita. Phys. Chem. Chem. Phys., **11**, 9850 (2009). DOI: 10.1039/B912178A

[53] R. Katoh, K. Suzuki, A. Furube, M. Kotani, K. Tokumaru. J. Phys. Chem. C., **113**, 2961 (2009). DOI: 10.1021/jp807684m

[54] B.P. Chandra, M.S. Khan, M.H. Ansari. Cryst. Res. Technol., **33**, 291 (1998). DOI: 10.1002/(SICI)1521-4079(1998)33:2¡291::AID-CRAT291¿3.0.CO;2-3

[55] J.-C.G. Bünzli, K.-L. Wong. J. Rare Earth., **36**, 1 (2018). DOI: 10.1016/j.jre.2017.09.005

[56] G.L. Sharipov, A.A. Tukhbatullin. J. Lumin., **215**, 116691 (2019). DOI: 10.1016/j.jlumin.2019.116691

[57] V.L. Ermolaev, E.B. Sveshnikova. Russ. Chem. Rev., **63**, 905 (1994). DOI: 10.1070/RC1994v063n11ABEH000125.

[58] G.L. Sharipov, A.A. Tukhbatullin, E.S. Mescheryakova. Opt. Mater., **52**, 44 (2016). DOI: 10.1016/j.optmat.2015.12.010

[59] I.G. Grevtseva, O.V. Ovchinnikov, M.S. Smirnov, K.S. Chirkov, A.N. Latyshev. Opt. i spektr., **132**, 675 (2024) (in Russian). DOI: 10.61011/OS.2024.06.58646.6194-24

Translated by A.Akhtyamov